UNIVERSITY OF CALIFORNIA SAN DIEGO

Role of STAT3/IFNg axis in promoting cancer stem cells (CSC)

A thesis submitted in partial satisfaction of the
requirements for the degree Master of Science

in

Bioengineering

by

Anushka Amarnath Poola

Committee in charge:

Professor Jack Bui, Chair
Professor Stephanie Fraley, Co-Chair
Professor Kevin King

2024

The thesis of Anushka Amarnath Poola is approved, and it is acceptable in quality and form for publication on microfilm and electronically.

University of California San Diego

2024

DEDICATION

To Amma, Nanna and Krithin.

TABLE OF CONTENTS

LIST OF FIGURES

LIST OF TABLES

Abbreviations

CSC cancer stem cells.

IFN interferon.

IFNg interferon gamma.

IFNGR interferon gamma receptor.

ISG interferon stimulated genes.

Flu fludarabine

NSG immunodeficient mice.

STAT signal transducer and activator of transcription.

ACKNOWLEDGEMENTS

I would like to sincerely thank Dr Jack Bui for guiding me throughout my master's journey and truly being a great PI. The environment he has created in the lab has made it a true pleasure to come in to work every day. His advice regarding how to approach and analyze science has been invaluable to me and they are skills I will take with me into my career here forward.

I owe the greatest thanks to Magalie Dosset, Wei Shan Chen and Lu Wang who have answered the endless questions that I have and for always being a great support system. A big shoutout to the entire Bui Lab team for being some of the nicest people: Sophia H, Sophia S, Marina, Rachel, Yipeng, Taian and Diane!

Lastly, I want to thank my family and friends for always motivating and encouraging me throughout this entire journey.

ABSTRACT OF THE THESIS

Role of STAT3/IFNg axis in promoting cancer stem cells (CSC)

by

Anushka Amarnath Poola

Master of Science in Bioengineering

University of California San Diego, 2024

Professor Jack Bui, Chair

Professor Stephanie Fraley, Co-Chair

Interferon-gamma (IFNγ) has emerged as a significant player in cancer biology, influencing stem-like cell populations in various cancer contexts. While IFNγ is used as a treatment option for cancer patients based on its anti-tumorigenic effects it is seen to have off target effects where it promotes tumorigenesis paradoxically. It has been shown that IFNg exposure increases the expression of certain cancer stem cell (CSC) markers. However, the mechanism of this is not yet understood. This study addresses this critical gap in being able to understand the role of IFNg experience in the regulation of cancer. It is hypothesized that IFNg treatment of breast cancer and sarcoma cells would induce stem-like phenotypes, but the

efficiency depends on whether STAT3 is activated by IFNg. So, if cells lacked STAT1, then IFNg should activate STAT3, and this could promote stemness, among other characteristics. This research has two areas of focus: in vitro and in vivo models of fibrosarcoma cell lines lacking or constituted with STAT1 and the effect of fludarabine (STAT1 inhibitor) on breast cancer cell lines. It is shown that IFNg exposure increases sphere formation and Sca1+/CD90- stem cell like marker expression in fibrosarcoma cells lacking STAT1 thereby potentially indicating that it is STAT3 behind these findings. In breast cancer models it was observed that fludarabine alone increase stem cell marker population as well as increases it even more synergistically with IFNg. These findings advance our understanding of the complex interplay of IFNg on the STAT1/STAT3 axis thereby effecting cancer stem cells in tumor biology.

Chapter 1

Introduction

Despite the extensive research aimed at unraveling and defining the mechanism of cancer development, growth, progression and then developing a variety of preventative measures and surgeries, cancer remains the top cause of death. [1]. Due to the heterogeneity seen in cancer it continues to be a global health challenge requiring the never-ending necessity for innovative treatment and management plans. Interferon (IFN) is a cytokine widely employed in immunotherapy due to its established anti-cancer effects. Initially recognized for its ability to inhibit cell proliferation and modulate immune responses, IFN has since been acknowledged for its cytotoxic effects and ability to hinder angiogenesis [2]. These multifaceted properties collectively establish IFN as a promising candidate for anticancer therapy

Cancer Stem Cells (CSCs)

CSCs are a small population within the tumor mass which possess enhanced self-renewal and differentiation capacities, allowing the cancer to initiate tumors, maintain cell growth and propagate. These cells have been implicated in tumor initiation, progression, metastasis, and chemotherapy resistance, making them a critical target for the development of effective cancer treatments because they increase the chances of a relapse depicted in Figure 1.1[3]. These cells may originate from either the genetic instability of tumor oncogenes or due to

the differentiation of stem cells. CSC model has emerged as this well-established idea as it seems to best explain and justify the versatile attributes of heterogenous tumor populations [4]. It is important to understand how we can modulate this to our advantage.

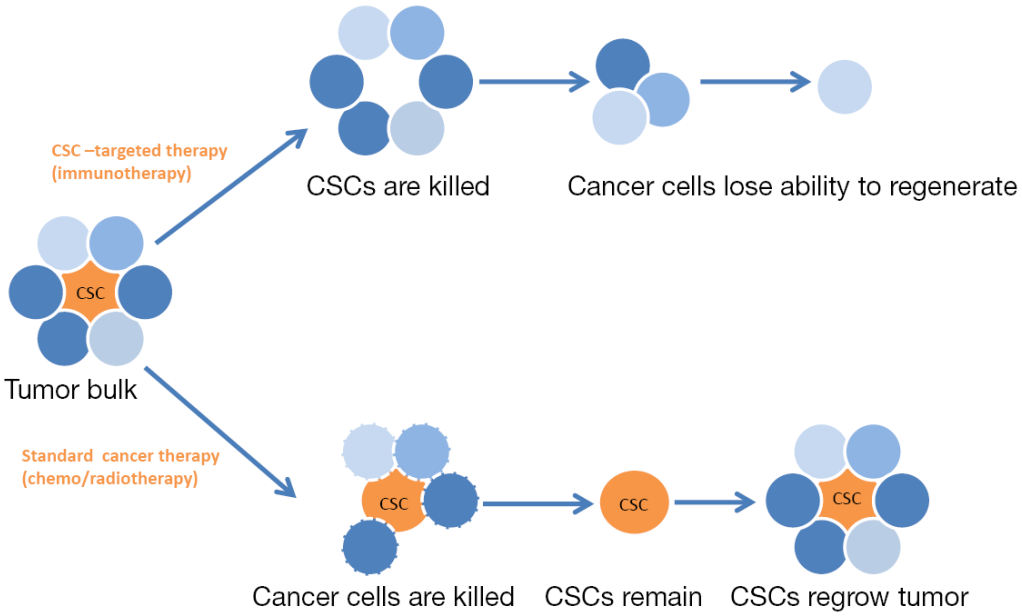

Figure 1.1. CSCs as a crucial target

CSC markers

To identify cells which could carry the risk for progression and maintenance of cancer and a potential relapse it is very important to define surface markers of CSCs in cancer patients. Several surface markers that characterize CSCs based on various different factors such as type of cancer, pre/post therapeutic period or stage of disease have been identified and correlated to diagnosis, therapy and prognosis[5]. In Table 1.1 a summary of some prominent CSC markers is provided as well as the ones studied in this project.

Table 1.1. Functions of CSC markers in tumor progression

Marker	Role
CD44	Proliferation, self-renewal and metastasis [6]
Sca1	Promote cell migration, decrease cell adhesion in vitro, regulate gene expression pathways [7]
CD90	Coordinate cell growth, metastasis and angiogenesis in tumors [8]
CD105	Proliferation and angiogenesis [9]
CD95	General growth promoting factor and mediate apoptosis induction [10]
Gal9	Inhibit T cell proliferation and metastatic progression [11]
CD133	High tumorgenicity and spheroid formation [5]

Interferons and their signaling pathway

Interferons (IFNs), play a vital role in the body's defense against viral infections and were initially identified based on this function of theirs. These small proteins are secreted by nucleated cells in response to viral infections or other stimuli. IFNs primarily act locally on nearby cells in a paracrine manner. IFNs also have significant immunomodulatory effects such as activating the immune system, inhibiting cell division and regulating cell growth and differentiation [2]. Initially classified based on their cellular origin as leukocyte, fibroblast, or immune IFN, IFNs are now recognized as a diverse family comprising more than 20 different proteins. IFNs are mainly classified into 3 groups

- Type I IFNs include interferon-alpha (IFN-α), interferon-beta (IFN-β) and other subtypes. They bind to their specific receptor. They are produced by most cells when there is a viral infection and bind to a shared cell-surface receptor. They are crucial for limiting the spread

of viral infections [13].

- Type II IFNs, which includes interferon-gamma (IFN-γ) are secreted by T cells and natural killer (NK) cells. Their signaling is through the IFNg receptor (IFNGR) bind to a different cell-surface receptor and activate macrophages and leukocytes specifically at sites of infection. Type II IFNs also enhance the effects of type I IFNs.
- Type III IFNs include interferon lambda (IFN-λ), which plays a significant role in controlling infections at mucosal surfaces, such as those in the respiratory and gastrointestinal tracts. Structurally these are seen to be similar to type 1 IFNs

Type I and type II interferons (IFNs) activate both common and distinct STAT (signal transducer and activator of transcription) complexes, which regulate the transcription of target genes. In addition to the classical Janus activated kinase (JAK)–STAT signaling pathways, both types of IFNs also trigger several other signaling cascades.

Type I interferons (IFNs) have a common receptor on human cell surfaces, known as the type I IFN receptor regardless of the type of type I IFN. This is composed of IFNAR1 and IFNAR2 subunits associated with tyrosine kinases TYK2 and JAK1, respectively. Whereas for type II IFN, IFN-γ, binds a distinct receptor composed of IFNGR1 and IFNGR2 subunits linked to JAK1 and JAK2, respectively. Activation of JAKs associated with the type I IFN receptor leads to STAT1 and STAT2 tyrosine phosphorylation, forming ISGF3 (IFN-stimulated gene factor) complexes [14]. This then translocate to the nucleus and bind to ISREs (IFN-stimulated response elements) to initiate gene transcription. Both type I and type II IFNs also induce STAT1 homodimers that translocate to the nucleus, binding GAS (IFN-γ-activated site)

elements in ISG promoters to initiate transcription of these genes [15].

Interferon gamma

Discovered in 1965, interferon gamma (IFN-γ) is a cytokine crucial for both innate and adaptive immune responses. It is mainly produced by T cells, NK cells, and NKT cells. IFN-γ plays essential roles in defending against infections and regulating the immune system. It exhibits powerful antiviral, antimicrobial, and antitumor effects, highlighting its importance in immune defense and disease control [16]. Additionally due to its anti-tumor effects in cell-mediated adaptive immune responses It is used in clinical settings to treat various cancers, though outcomes have been variable and associated with significant side effects [17]. While IFN-γ is recognized for its role in tumor immune surveillance, recent studies have also indicated potential protumorigenic effects in specific contexts. And through this project we hope to gain findings relevant to this.

Contradictory effects of interferon gamma

The role of IFN-γ in cancer host responses has been extensively studied and has revealed that it is highly involved in immune surveillance and has a correlation with tumor regression in immunotherapy. This cytokine is also known to exerts direct antitumor effects by inhibiting angiogenesis, suppressing proliferation, sensitizing tumor cells to apoptosis, enhancing MHC class I and II expression, and stimulating antitumor immune responses [18]. Specifically, it is known to exert this through this through STAT 1 signaling [19]. However, clinical efficacy has shown variability across different cancer types.

In studies involving recurrent superficial transitional bladder carcinoma, intravesical

IFN-γ instillations effectively reduced cancer recurrence, correlating with increased infiltration of T cells, NK cells, ICAM-1+ B cells, and HLA-DR+ cells within tumors [20]. Enhanced IFN-γ-induced HLA-DR expression has been linked to improved prognosis in colorectal cancer. Ovarian cancer, a significant cause of cancer-related mortality, has been targeted with cytokine therapies due to the presence of intratumoral IFN-γ-producing CD3+ T cells associated with better outcomes.

In clinical settings, IFN-γ has shown synergistic effects with platinum-based chemotherapy against ovarian cancer [21], demonstrating anti-proliferative and apoptotic-inducing properties. Intraperitoneal IFN-γ administration has also elicited anti-tumor responses. Recent randomized trials have highlighted improved complete response rates and progression-free survival with subcutaneous IFN-γ in combination with cisplatin [22]. However, not all trials have been successful; a phase III study combining IFN-γ with carboplatin/paclitaxel in ovarian and peritoneal carcinoma was terminated early due to significantly shorter survival rates and increased adverse events compared to chemotherapy alone [23].

Contradictingly we also see that IFNg can have pro tumorigenic effects depending on the cellular and molecular microenvironment. The contrast in their effect is summarized in Table 1.2.

Table 1.2. Anti- and pro- CSC effects of IFN type 1 and type 2[15]

Anti-CSC effects	Pro-CSC effects
IFN-I	
Decreased expression of stem-like markers and/or pluripotency genes (1–3)	Increased expression of stem-like markers and/or pluripotency genes (4–6)
Reduced self-renewal capacity (1, 2, 7–10)	Increased self-renewal capacity (4–6)
Reduced tumorigenic potential (1, 7, 9)	Increased tumorigenic potential (5, 6)
Reduced proliferation (7, 9, 10)	Chemoresistance (6)
Reduced metastatic potential (9)	Increased migratory/invasive and/or metastatic capacities (3, 6)
	Induction of dormancy (11)
IFN-II	
Reduced self-renewal capacity (14)	Increased self-renewal capacity (12, 15)
Reduced tumorigenic potential (14)	Increased tumorigenic potential (13)
Reduced migratory/invasive capacities (16)	Activation of EMT and/or migration/invasion (12, 15)
	Increased expression of stem-like markers and/or pluripotency genes (12, 13)
	Increased metastatic potential (15, 17–22)
	Chemoresistance (15)
	Induction of dormancy (23–25)

Low doses of IFN-γ can help tumor cells survive in circulation and increase their metastatic potential [24] IFN-γ has also been shown to cause apoptosis in tumor-specific T cells, this has a direct effect on weakening anti-tumor immunity [25]. IFN-γ can promote B7H4 and PDL1 expression (B7H4 and PDL1 are transmembrane proteins and immune checkpoint ligands which promote tumor progression by inhibiting T cell immunity) in colorectal cancer cells, which can inhibit cytotoxic T cells [26]. IFN-γ can cause tumor cells, monocytes, endothelial cells, and fibroblasts to secrete CXCL11, which binds to CXCR7 and promotes tumor growth and angiogenesis [27].

These findings highlight the complexity of IFN-γ's therapeutic potential and show the requirement for further research to optimize clinical applications in cancer treatment.

Role of Fludarabine to inhibit STAT 1

Fludarabine, a prodrug converted into the nucleoside 9-β-D-arabinosyl-2-fluoroadenine (F-ara-A), primarily accumulates within cells as its active form, F-ara-ATP, following a series of enzymatic conversion [28]. Its mechanisms of action predominantly target DNA processes, inhibiting ribonucleotide reductase, incorporating into DNA to impede further polymerization, and hindering DNA ligase and DNA primase activities. It is most commonly used to treat B cell chronic lymphocytic leukemia [29].

Of particular interest in the context of the JAK-STAT pathway, Fludarabine inhibits signal transducer and activator of transcription 1 (STAT1) in both normal and cancer cells. This inhibition prevents cytokine-induced activation of STAT1 and subsequent STAT1-dependent gene transcription [30]. Fludarabine achieves this by binding to the SH2-phosphotyrosine binding pocket of STAT1, thereby obstructing its interaction with IFN receptors, phosphorylation at Tyr701, and formation of homo- and/or heterodimers. Additionally, Fludarabine can induce specific depletion of STAT1 protein and mRNA levels. Thus, it can block interferon signaling [31].

My research and hypothesis based on literature review

Previous research has explored the contradicting effects that IFNg seems to have on promoting/inhibiting CSCs. IFNs have been shown to influence CSC biology and hence its important to gain a better understanding of its therapeutic potential.

In this study we utilized different H74 fibrosarcoma cell lines one which had STAT1 knocked

out and the other which was reconstitute with STAT1 to investigate the effects of IFN experience on the expression of CSC markers in vitro and in vivo models. We also test the effect of fludarabine on breast cancer cell lines to explore similar concepts. Based on these models we hypothesize that IFNg treatment of breast cancer and sarcoma cells would induce stem-like phenotypes, but the efficiency depends on whether STAT3 is activated by IFNg. So, if cells lacked STAT1, then IFNg should activate STAT3, and this could promote stemness, among other characteristics

.

Chapter 2

Results

2.1 Study of H74 sarcoma cell line *invitro* and *invivo*

2.1.1 IFNg treatment increases sphere formation in STAT1-deficient cells

Based on unpublished data from our lab it has been demonstrated that interferon-gamma (IFNγ) expands the population of stem-like cells in various cancer cell lines, including HMLE, T47D, MDA-MB-231, SKOV-3, and F244. These observations were made through time-course experiments with measurements taken over a range of time points, from hourly measurements during the first 24 hours to extended incubation periods lasting up to 14 days. Increased exposure to IFNγ, particularly with longer incubation times, correlated with an augmentation of the "stem-like" population identified by combinations of specific cell specific surface markers. Nevertheless, this effect did not occur with all cell lines, and it was not known why some cell lines responded and some did not.

As discussed earlier the effect of IFNγ on tumor growth is a topic of debate with conflicting evidence in the literature, in this study we aim to investigate whether IFNγ influences STAT3 signaling, as opposed to it activating STAT1 signaling pathway which is well established. We hypothesize that in the absence of STAT1, IFNγ preferentially activates

STAT3, leading to the upregulation of the stem-like cell population (known to be associated with Stat3) and potentially promoting tumorigenic effects. Thus, the cell lines that responded to IFNg by increasing CSC properties might preferentially activate STAT3 vs STAT1 downstream of IFNg.

One way to assess the stem-like properties of cells is a sphere formation assay. This assay mimics the stem cell microenvironment found in vivo by culturing cells in non-adherent conditions. This facilitates the formation of spheres enriched for stem cells, allowing us to evaluate their capacity for proliferation, survival, and differentiation all of which are key characteristics to define stem cell likeness.

In this experiment we used three different cell lines: H74 par, derived from a STAT1-deficient fibrosarcoma; H74 RVE, a clone of H74 par transduced with an empty retroviral vector; and H74 RVS, a clone of H74 par reintroduced with STAT1 via a retroviral vector. We hypothesized that H74 par and H74 RVE cells would show an increased sphere formation compared to H74 RVS cells, and that IFNγ treatment would further enhance this effect since without STAT1, IFNg would stimulate STAT3.

As expected, shown in Figure 2.1, H74 par and H74 RVE cell lines formed significantly more spheres compared to H74 RVS cells, supporting the established role of Stat1 in suppressing sphere formation. Interestingly, IFNγ treatment did not significantly alter sphere formation in H74 par cells. However, H74 RVS cells displayed a reduction in spheres upon IFNγ treatment, consistent with existing literature suggesting that IFNγ-induced Stat1 activation mediates anti-tumor effects.

As expected, IFNγ treatment led to an increase in sphere formation in the STAT1-deficient H74 RVE cell line. This suggests an alternative effect that may be taking place where

IFNγ is activating Stat3 in the absence of Stat1, in turn increasing the stem cell-like population. These findings however warrant further investigation to determine the specific molecular mechanisms by which IFNγ could be activating Stat3 in the absence of Stat1, resulting in the presented findings

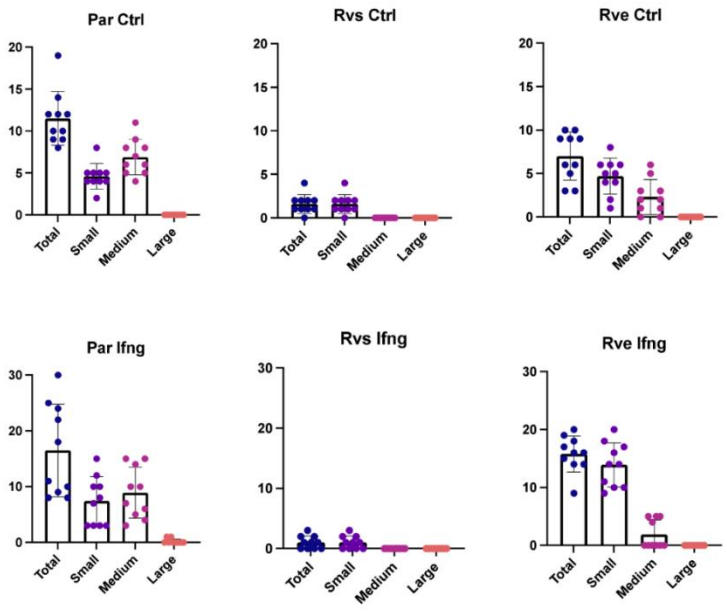

Figure 2.1. Sphere formation in STAT1 deficient and reconstituted H74 fibrosarcoma cells and the effect of IFNg on its activity

2.1.2 Growth Differences between H74 RVE and H74 RVS cell lines in WT and NSG mice in vivo

This experiment was focused on determining whether H74 RVE cells exhibit faster in vivo growth compared to H74 RVS cells, and whether IFNg induces accelerated growth, a pro-tumor-like effect, and that the cytokine is activating STAT3 in the absence of STAT1, cells were injected into both wild-type and immunodeficient mice in an attempt to demonstrate this.

In wild-type mice, we hypothesized that H74 RVE cells would demonstrate faster growth than H74 RVS cells. Conversely, in immunodeficient mice, any observed growth differences were expected to be minimal due to suppressed immune responses. Additionally, comparisons between wild-type and immunodeficient mice were expected to reveal slower growth in wild-type mice due to initial tumor rejection mechanisms.

Tumor size was monitored periodically following cell injection. Consistent with our hypotheses, in immunodeficient mice, there was no significant difference in tumor growth between H74 RVE and H74 RVS cells, as shown in Figure 2.2. A slight increase in RVS tumor growth relative to RVE was noted. In wild-type mice, H74 RVE cells indeed exhibited slower growth compared to immunodeficient mice. Notably, H74 RVS cells injected into wild-type mice were completely rejected approximately 15 days post-injection.

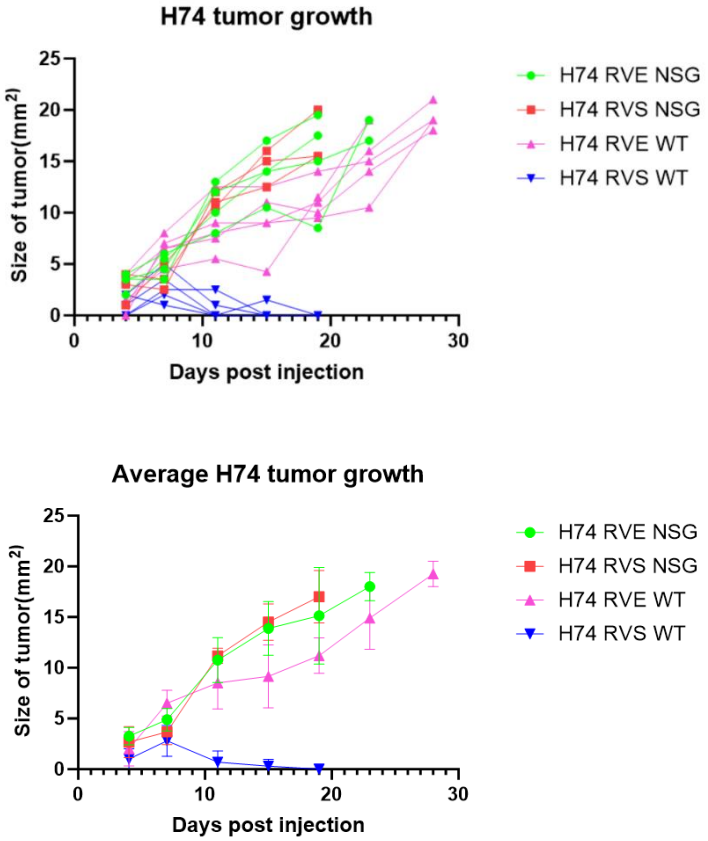

Figure 2.2. H74 RVE and H74 RVS tumor growth in wildtype and immunodeficient mice

2.1.3 STAT 1 Deficient cells generate more Sca 1+ and CD90- CSCs

My hypothesis here explored whether IFN experienced STAT 1 deficient (RVE) H74

tumors i.e the tumors harvested from the immunocompetent mice would present more CSC surface markers. And also we were testing the hypothesis that the STAT1 deficient tumors had more CSC markers in comparison to the STAT1 reconstituted (RVS) tumors. Tumor cells were gated on the CD45- population the lack of which is indicative of tumor cells. Within this population we then gated on Sca1 + and CD90- population which is the stem cell like defined population. It was observed (Figure 2.3) that the RVE tumors both from immunocompetent and immunodeficient mice had a greater percentage of this population than the RVS from immunodeficient mice (RVS from immunocompetent mice not considered as completely rejected in vivo). This could signify that the IFNg produced by the cells which are present in the immunocompetent mice and absent in the immunodeficient mice are activating STAT3 in the absence of STAT1 in accordance with out hypothesis. Also as seen in Figure 2.3, between the RVE tumors from immunodeficient and immunocompetent mice we see that the average levels across all samples are not significantly different. However, looking at each sample individually RVE immunodeficient tumors seemed to have slightly elevated levels of this population. Within this Sca1+ CD90- CSC like population we further analyzed (Figure 2.4) other surface markers of interest namely CD105 and CD95. It was observed that the RVE tumors do not express CD105 and the RVS tumors have slightly elevated levels. It was also seen that the CD95 expression remained unchanged across all categories.

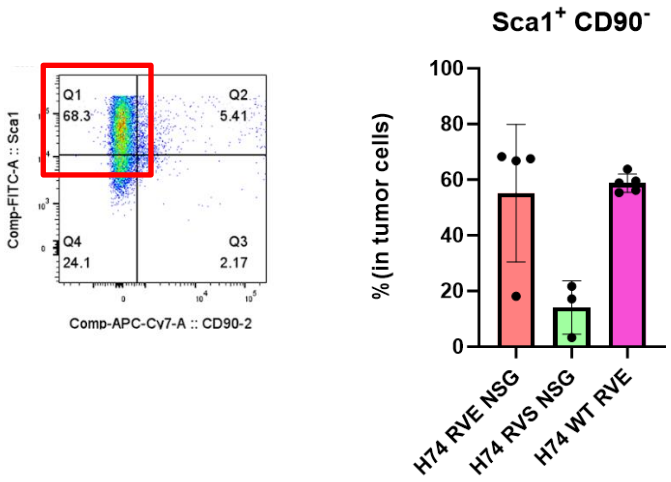

Figure 2.3. Sca1+/CD90- expression in H74RVE and H74 RVS tumors in wildtype and immunodeficient mice and Flow Cytometry plot depicting the population of interest

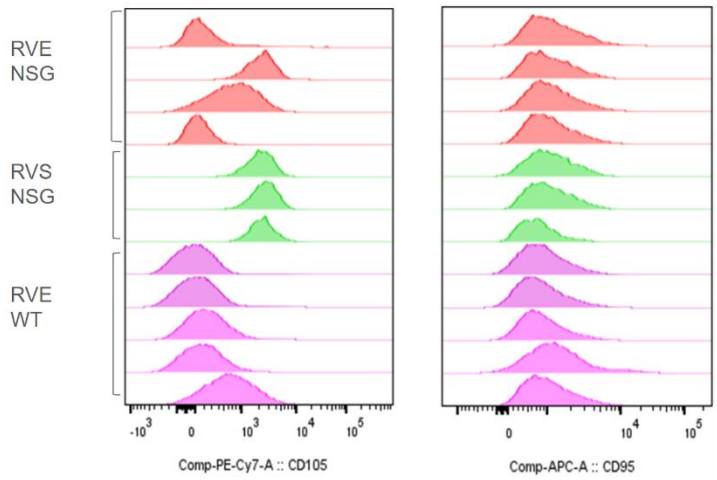

Figure 2.4. CD105 and CD95 expression in H74RVE and H74 RVS tumors in wildtype and immunodeficient mice

Post analysis the remaining harvested tumors cells were cultured for 14 days and amplified and again reanalyzed by flow cytometry in a similar manner for the same staining panel. Interestingly the Sca1+/CD90- population across the board had increased within the CD45- gated population. Specifically in the WT RVE group we observed an average increase from

55.4% to 93.1% as shown in Figure 2.4. Based on these results CSC like population improved with the amplification suggesting that the CSC are potentially more resistant and surviving while in culture. And this increase led to a significant difference between this group and RVE NSG which remained unchanged at an average of 63%. Again, within this population we also checked to see if there was any influence on CD105 and CD95 expression. CD105 expression remained unchanged and interestingly the outliers within the group seemed to have gained an expression more like other members of the group. The CD95 expression seemed to have slightly increased, and the profile showed some difference. Further investigation is required to elucidate the exact meaning and draw a direct connection back to our hypothesis.

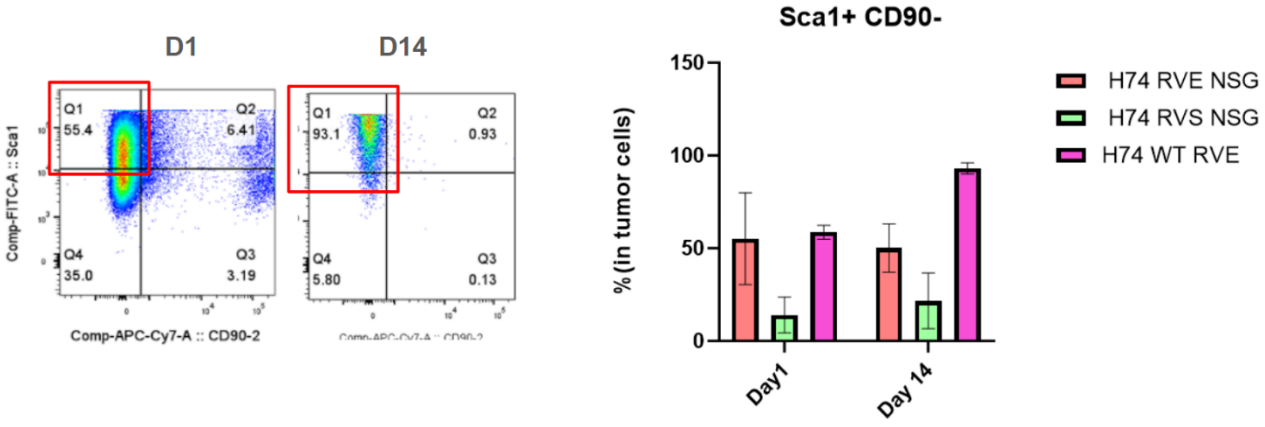

Figure 2.5. Sca1+/CD90- expression in H74RVE and H74 RVS tumors in wildtype and immunodeficient mice post 14 days amplification depicting a significant increase in the CSC population H74 RVE wildtype mice , highlighting potential IFNg-related influence

2.1.4 Investigating other CSC surface markers within H74 RVE and RVS tumor cells

Next, I examined other potential surface markers that may be able to define the fibrosarcoma stem cell like population. We wished to see similar patterns as previously found with the Sca1+/CD90- data and hence made similar hypotheses. Similarly to the discussion above we gated on CD45- population so that we can exclusively analyze the tumor cells. Within the tumor cell population, we specifically gated on the CD44hi and CD24lo population. It was seen that throughout all groups as depicted in Figure 2.5 there was no significant difference between any of the groups with all of them around 80% and mainly there being no difference between RVE and RVS tumor cells. This indicates that CD44 and CD24 may not be good markers for this cell line and hence cannot be used to define stem cell likeness. Within this initially assumed stem cell like population we also investigated galectin9 and MHC 1 expression. Similarly, we saw no significant differences in their expression across the three groups as show in Figure 2.6. These results point us towards the necessity of being able to find more representative markers for fibrosarcoma CSC populations.

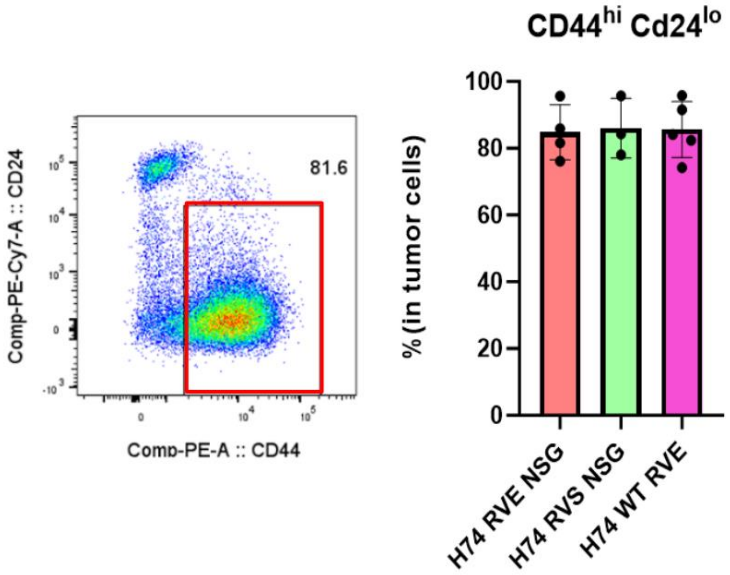

Figure 2.6. No significant differences observed in CD44hi/CD24lo expression in H74 RVE and H74 RVS tumors in wildtype and immunodeficient

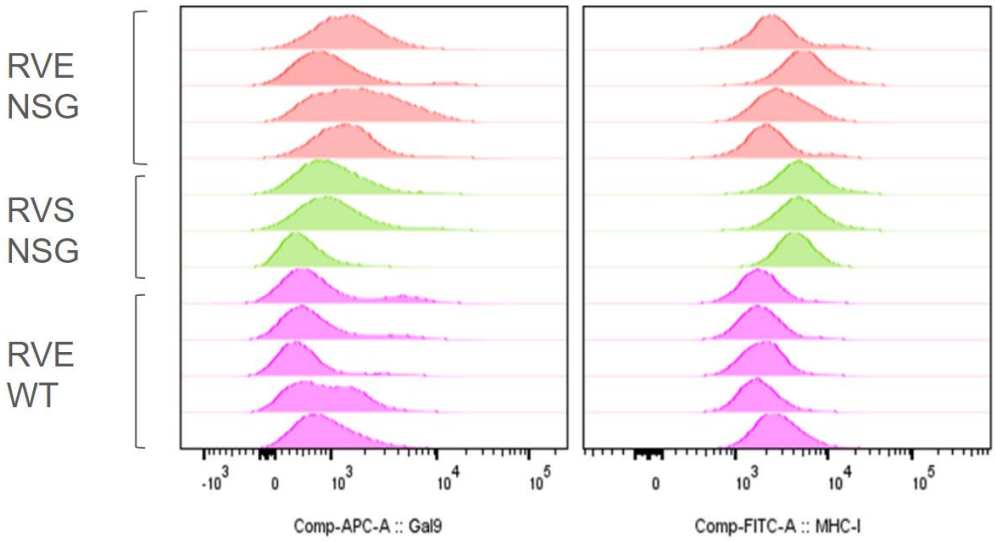

Figure 2.7. Gal9 and MHC I expression within the CD44hi/CD24lo population in H74RVE and H74 RVS tumors in wildtype and immunodeficient

2.1.5 Difference in generation of spheres between isolated H74 tumor cells and the same cells after 14 days amplification

We then wanted to explore the sphere forming capacity of these cell lines. In light of previous findings, we hypothesized that the H74 RVE WT tumor cells should form more spheres among all the three groups. And between H74 RVE NSG and H74 RVS NSG there would not be a difference in sphere formation in terms of number as there was no interferon exposure to the cells. We also wanted to investigate what effect this might have on the size of the spheres that are formed. Interestingly on the day of harvest the batch of cells that were seeded post 14 days of the assay being conducted the results did not seem to be in line with this hypothesis. It was observed that the H74 RVS NSG cell lines gave rise to the most number of spheres. It was almost 4-fold more than the RVE WT and RVE NSG, which was unexpected. The reason for this observation is yet to be understood. It was also seen that in terms of sizes of sphere across small, medium and large these also formed almost 1.5-fold more. However, neglecting this particular group and just comparing the RVE NSG and RVE WT we did observe more spheres

in terms of both the total number and amongst the different size of spheres. This is in line with the hypothesis as the RVE WT are IFNg exposed and has increased the stem cell like population.

In a similar way with the previous studies, we also did culture the tumor cells over 14 days, passaging them when required to maintain them. And since we did observe an increase in the CSC Sca1+/CD90- population then maybe post the 14-day period we would see results more like our hypothesis. And indeed, this was what was observed. Overall, we did see more spheres being formed for RVE (both WT and NSG) as compared to the RVS. On average, RVE WT formed a total of 50 spheres, RVE NSG around 25 and RVS at the lowest around 18. Interestingly though if we compare the RVS total spheres formed on D1 and D14 we saw a decrease. One potential reason for this could be that in the initial cells seeded were not pure tumor cells they also did have some immune cells with most likely a large population being macrophages and it was these macrophages that were aiding the sphere formation. A potential future experiment for this would potentially analyze the gene expression within these spheres to specifically show that STAT 3 is upregulated in the groups where there are more spheres formed to be able to draw a direct correlation back to our hypothesis and to rule out any external factors that may be aiding in this.

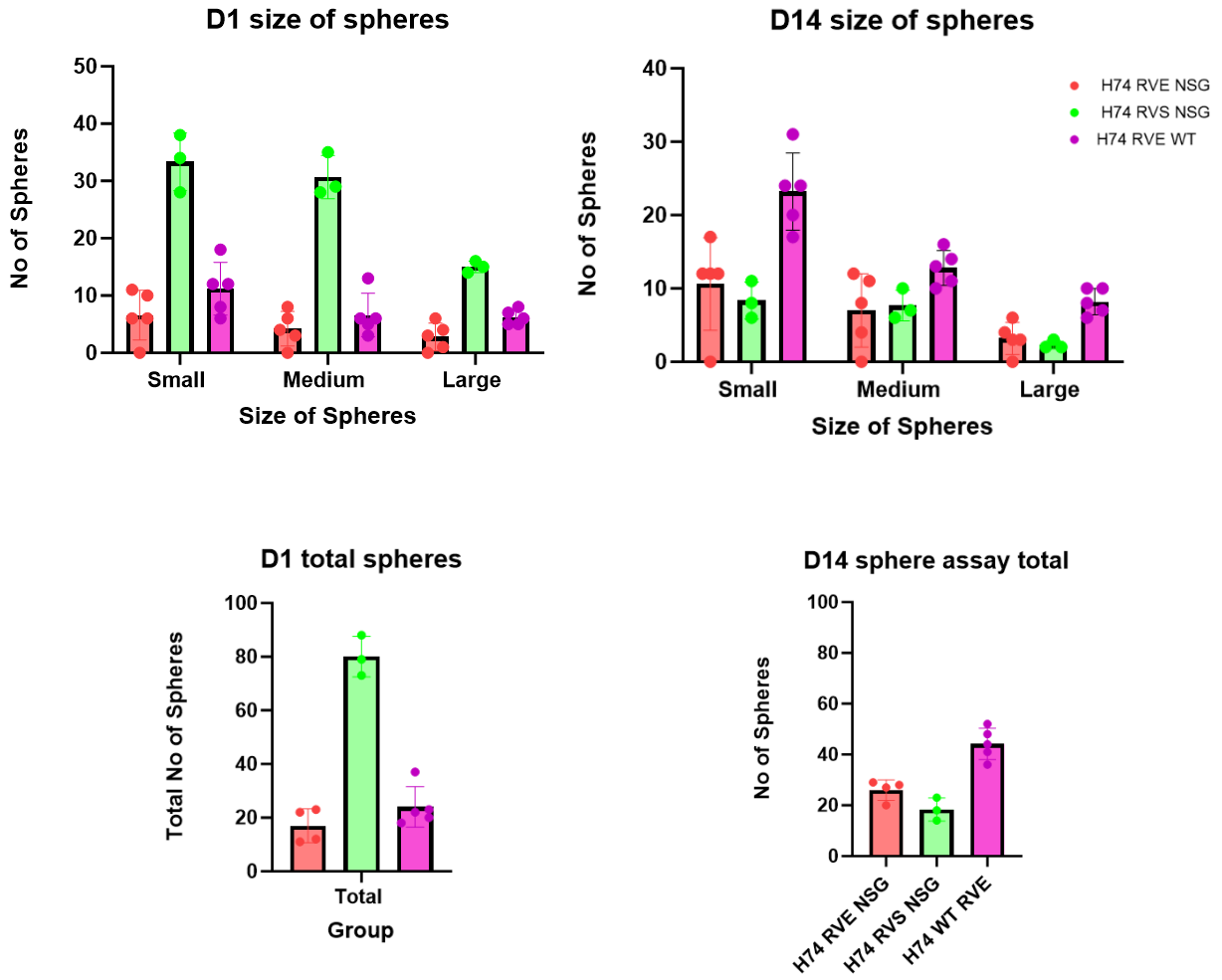

Figure 2.8. Sphere formation assay from H74 RVE and H74 RVS tumors in wildtype and immunodeficient demonstrating that after 14 days H74 RVE isolated from WT mice and amplified invitro generated more spheres than other groups

2.2 Study of the involvement of IFNg/STAT1/STAT3 axis in breast cancer cell lines in vitro

2.2.1 Effect of Fludarabine and IFNg in stimulation the Sca1+/CD90- CSC population

These experiments were focused on understanding whether the commonly used therapeutic drug fludarabine which is known to be a STAT 1 inhibitor has any effect on influencing CSC promotion. And once STAT1 has been inhibited when treated with IFNg whether we see an increase in the CSC like population. To begin establishing a baseline and to

observe whether IFNg without STAT1 being inhibited could induce the Sca1+/CD90- population. We treated 4T1 and Py230 cells with 1000U/mL of IFNg for 24 hours. In 4T1 we observed a 2 fold increase in the population of interest reaching around 60% when treated with IFNg. In py230 we saw it increase from 8% to 74%. From this we can infer that even in spite of STAT1 being present STAT3 is being activated by the IFNg leading us to the observed results. It would be good to know what the inherent levels of expression of STAT1 and STAT3 in these cells are to begin with. We then wanted to see what effect Fludarabine had on the cells when it was inhibiting STAT1. We tested 5 different doses of the drug on 4T1 cells. 0uM (control), 25uM, 50uM, 75uM and 100uM. It looked like with a higher dosage of the drug i.e. with 75uM and 100uM there was an upregulation of the CSC like population compared to the control i.e. no drug treatment. This was after 24 hours of treatment. It was also observed that 25uM and 50uM also exhibited a slight increase in the CSC like population however it was not significantly different from the control. And finally, we wished to check once STAT1 had been inhibited by Fludarabine whether IFNg could increase the CSC like population even further. It was expected that with higher amounts of drug the extent of STAT 1 inhibition would be increased therefore when treated with IFNg. We observed a synergistic effect between fludarabine and IFNg in inducing the Sca1+/CD90- CSC population. Interestingly though for the higher concentrations of drug we observed a lower induction even lower than the control which was just interferon. One possible explanation for this could be that at the higher concentrations it was inducing cell apoptosis which has been previously described in literature. The lower concentrations 25uM and 50uM increased the population percentage above the control with 50uM reaching the highest around 86%. Through this we can arrive closer at the conclusion that STAT3 is being stimulated by IFNg in the absence of STAT 1 and causing the upregulation of the CSC population. However, it is necessary to be able to show these findings across other cell lines as well as marker populations more specific to the breast cancer phenotype.

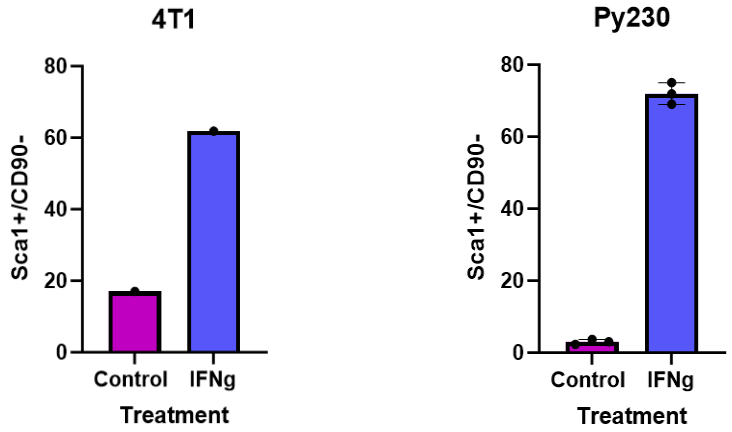

Figure 2.9. IFNg at 1000U/mL is seen to stimulate Sca1+/CD90- population in 4T1 and Py230 breast cancer cell lines.

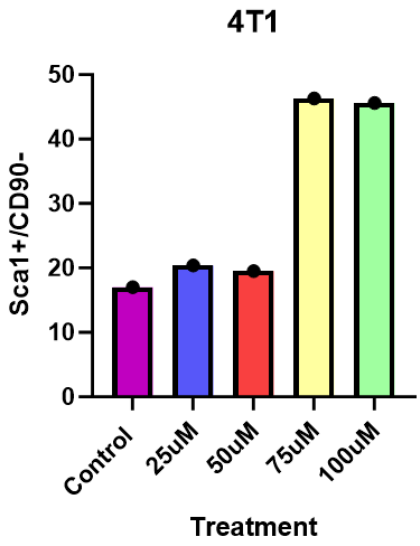

Figure 2.10. Fludarabine treatment alone on 4T1 breast cancer cells for 24 hours is seen to stimulate Sca1+/CD90- population with higher doses inducing it more.

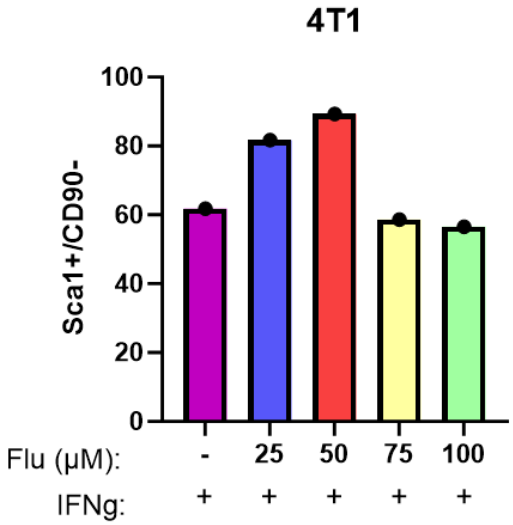

Figure 2.11. Synergistic effect observed between fludarabine and IFNg to induce Sca1+/CD90- CSC population in 4T1 breast cancer cells

Chapter 3

Discussion

Study of H74 sarcoma cell line invitro

We used 2 main cell lines: H74 RVE (STAT1 deficient) and H74 RVS (STAT1 reconstituted) which will help us understand whether interferon gamma experience on cells will activate STAT3 in the absence/lower levels of STAT1. The presented study investigates the expression of particular CSC markers in the cells from harvested tumors from wildtype and immunodeficient mice. It also aims to gain an understanding of the sphere forming capacities of these cells. This assay mimics the stem cell microenvironment found in vivo by culturing cells in non-adherent conditions. This facilitates the formation of spheres enriched for stem cells, allowing us to evaluate their capacity for proliferation, survival, and differentiation all of which are key characteristics to define stem cell likeness.

Interestingly, IFNγ treatment did not alter sphere forming capacity in H74 par cells, indicating that STAT1 deficiency alone may suffice to enhance stem-likeness irrespective of IFNγ. However it was observed that IFNγ experience of the cells significantly increased sphere formation in H74 RVE cells the most compared to other groups , further highlighting a potential shift towards a more stem-like phenotype due to STAT3 activation under STAT1-deficient condition

These findings suggest a dual role for IFNγ depending on the STAT1 status of the cells. In STAT1-deficient contexts, such as H74 RVE cells, IFNγ may activate alternative signaling pathways, potentially involving STAT3, to promote stemness. This aligns with our hypothesis that in the absence of STAT1, IFNγ could preferentially activate STAT3, contributing to the expansion of the stem-like cell population observed in our experiments.

Further investigation into the specific molecular mechanisms by which IFNγ activates STAT3 in STAT1-deficient settings is warranted.

In vivo Experiment

Flow cytometry analysis gated on the CD45- population revealed that both immunocompetent and immunodeficient RVE tumors exhibited a higher percentage of the Sca1+/CD90- CSC-like population compared to immunodeficient RVS tumors (Figure 2.3). This suggests that IFNγ, likely produced by immune cells present in immunocompetent hosts, activates STAT3 in the absence of STAT1, promoting a stem-like phenotype in tumor cells.

Further analysis of CSC markers within the Sca1+/CD90- population (Figure 2.4) showed that RVE tumors generally lacked CD105 expression, whereas RVS tumors displayed slightly elevated levels. From this we can infer that CD105 may play some role in preventing the CSCs from developing ie having a protective effect in fibrosarcoma.

Interestingly the sphere assay conducted at this same time point demonstrated that RVS formed more spheres which is not in line with the flow data. One reason for this could be that the tumor cells were not purified before seeding them into the assay and there were immune cells present. It has been seen in literature that immune cells specifically macrophages can influence sphere formation and particularly those involved in the tumor microenvironment can modulate the behavior and characteristics of CSCs.

Subsequent culture and amplification of harvested tumor cells for 14 days revealed a significant increase in the Sca1+/CD90- population, particularly notable in immunocompetent RVE tumors where the average percentage rose substantially (Figure 2.4). This indicates a survival advantage and potential enrichment of CSCs under prolonged culture conditions . This is also reflected in the tumor cell sphere assay conducted as we see better sphere formation there.

The observed enrichment of CSC-like populations in STAT1-deficient tumors, particularly in the presence of immune-derived IFNγ, highlights a mechanism where STAT3 activation compensates for STAT1 loss to sustain stemness traits.

Fludarabine effect on inducing STAT3 in breast cancer cell lines

The observed results suggest complex interactions between interferon-gamma (IFNγ), fludarabine (a STAT1 inhibitor), and cancer stem cell (CSC) populations, particularly in 4T1 cell lines.

The observed increase in the Sca1+/CD90- CSC population in 4T1 and Py230 cells after treatment with IFNγ despite STAT1 inhibition (Figure 2.1) suggests that IFNγ is indeed stimulating STAT3 in the absence of STAT1. This activation of STAT3 may contribute to the observed increase in CSC-like characteristics, including enhanced self-renewal and survival capabilities.

At higher concentrations (75uM and 100uM), fludarabine upregulates the CSC-like population compared to the control (0uM), indicating a dose-dependent effect. The slight increase observed at lower concentrations (25uM and 50uM) suggests a threshold effect, where STAT1 inhibition may not be sufficient to fully enhance CSC-like characteristics unless complemented by IFNγ-mediated STAT3 activation.

The combination of fludarabine-induced STAT1 inhibition and subsequent IFNγ treatment

resulted in a synergistic increase in the Sca1+/CD90- CSC population. This synergism was most pronounced at intermediate concentrations of fludarabine (25uM and 50uM), where the CSC population percentage exceeded that of both control and single-agent treatments.

Interestingly, at higher concentrations of fludarabine (75uM and 100uM), the induction of CSC-like populations decreased, potentially due to cytotoxic effects, including apoptosis induction, as described in the literature.

Different cell lines and phenotypes may exhibit varying responses to IFNγ and STAT1 inhibition, necessitating broader validation across multiple models.

Future Directions

In terms of being able to indeed prove that it is STAT3 that is being upregulated. It would be essential to show there is an increase in STAT3 phosphorylation which would be able to confirm this. Additionally, gene silencing experiments and overexpression employing techniques such as siRNA-mediated knockdown or CRISPR/Cas9 gene editing for silencing, and plasmid or viral vector-based gene delivery for overexpression can be conducted as well. The outcomes of these experiments would clarify the roles of these genes in regulating stem-like characteristics of the cells.

Overall, the next steps of this research is to provide a more detailed picture of the direct interplay between IFN treatment and activation of STAT 3 potentially displaying an increased phosphorylation, gene expression, and cellular characteristics in the context of tumor biology. This multifaceted approach promises to contribute valuable insights to the field and guide the development of more effective cancer therapies.

Chapter 4

Materials and Methods

Cell Lines

H74 RVE, H74 RVS, 4T1, and Py230 cell lines were maintained by passaging cells when 80% confluent. Passaging was done by trypsinizing the cells for 5 minutes at 37°C or until cell detachment could be observed under the microscope. Cells were then washed in their appropriate media and then reseeded in fresh medium and placed in the incubator at 37°C. Excess cells were frozen down by resuspending in their media and 10% DMSO in cryovials for future use.

Media Preparation (CR-10 media and Py230 media)

500 ml of RPMI 1640 medium (ThermoFisher Scientific) was used as a base for the culture of H74 RVE, H74 RVS, 4T1 cell lines, and tumor cells. This was supplemented with 50 ml of fetal bovine serum, 5 ml of 200mM sodium pyruvate, 5 ml of 200mM L-glutamine, 2.5 ml of 7.5% sodium bicarbonate, 0.5 ml of 55mM b=mercaptoethanol and 5 ml non-essential amino acids. 5ml of pen/strep was added as a bacterial contamination control.

500ml of Ham's F-12K (Kaighn's) Medium (ThermoFisher Scientific) was used as the base for the culture of Py230 cells. This was supplemented with 50ml of fetal bovine serum, 5ml of anti-anti was added as a bacterial and mycotic contamination control, and 500ul of mito was added as well.

Sphere Assay

H74 cell lines (Par, Rvs and Rve) cells were prepared for the sphere assay by first trypsinizing them from 80% confluent T-75 flasks yielding around 7 million cells per cell line. Once harvested the cells were washed 3 times in ice-cold PBS to remove any trace of serum that might still be present. The cells were counted and resuspended to 1 million cells per mL in sphere media (1% N2 supplement, bFGF and EGF). 30,000 cells were seeded into a 24 well untreated plate along with 1mL of the sphere media. Every other day the bFGF and EGF supplement was added. This was monitored for a period of 14 days. On the 14th day, the spheres were counted in 5 hi power fields (12, 3, 6 9 o'clock, and the center of the well).

Preparing Cells for Injection

H74 RVE and H74 RVS cells were prepared for subcutaneous injection into mice with a focus on maintaining high cell viability and minimizing impact on their growth phenotype. The cells were harvested from three T175 flasks per cell line, each flask being 70-80% confluent, resulting in approximately 12 million cells per flask.

To prepare for injection, the cells were detached from the flasks using trypsin and collected in a sterile conical tube to create a uniform single-cell suspension in CR-10 media. The cell suspension was then centrifuged to form a pellet, which was washed with media and subsequently washed three times with ice-cold HBSS (containing calcium and magnesium) to remove residual media and trypsin.

After washing, the cells were resuspended in CR-10 media to achieve a final concentration of 10 million cells per mL. For injection, 100 µL of this suspension, containing 1

million cells, was subcutaneously injected into the right flank of each mouse. This protocol was carried out for 9 mice injected with H74 RVE cells and 8 mice injected with H74 RVS cells, encompassing both wild-type and immunodeficient mice as experimental conditions required.

Tumor Harvest and Processing

Tumors were harvested from mice when they reached an average size ranging from 15 mm^2 x 15 mm^2 to 20 mm^2 x 20 mm^2. The mice were euthanized by cervical dislocation after both the mice and the equipment were sterilized with ethanol. A careful incision was made on the right flank, and the tumor was excised while ensuring separation from the surrounding fat tissue.

Immediately after excision, the tumor was transferred into a sterile conical flask containing 5 mL of CR-10 media and placed on ice to maintain its integrity until all tumors were harvested. The entire process of handling tumors was conducted within a laminar flow tissue culture hood to ensure a sterile environment during cell extraction.

Once all tumors were collected, each tumor was minced into small pieces measuring approximately 1 mm^2 x 1 mm^2 using sterilized razor blades in a sterile petri dish. The minced tumor pieces were carefully rinsed off the petri dish using a 2 mg/mL collagenase type I solution, which was collected into a sterile conical tube. The tube containing the minced tumor and collagenase solution was then placed in a 37°C water bath and incubated for 45 minutes, with periodic mixing by gentle inversion of the tube.

Following the incubation period, the tumor suspension was homogenized using a 60 µm filter and CR-10 media to ensure a uniform single-cell suspension. The filtrate was then centrifuged at 300g for 10 minutes at room temperature. After centrifugation, the supernatant containing cell debris and collagenase was carefully decanted, leaving behind a cell pellet at the bottom of the tube.

The cell pellet was gently resuspended in an appropriate volume of CR-10 media. Subsequently, the cell suspension was carefully transferred to a sterile cell counting chamber, and the cells were counted using a microscope to determine the concentration. The counted cells were then diluted or adjusted as necessary for further experimental procedures or analyses.

Expansion of Tumor Cell Lines

Once the cells were obtained from each of the tumors they were seeded into T-75 flasks with CR-10 media to allow for the expansion. At this time cells were also preserved by freezing them down. They were resuspended in CR-10 media and 10% DMSO in cryovials for the future. The cells seeded into the T-75 flasks were allowed to culture for 14 days. They were passaged in between to maintain the cell lines during this period. On day 14 the cells were harvested for the necessary studies as well as frozen down at this time point for future use.

Flow Cytometry for Surface Marker Analysis

The tumor cells once harvested at the necessary time points were prepared for flow cytometry. 500,000 cells were added to FACS tubes. The cells were washed twice with facs buffer at 500g for 5min at 4C. The cells were stained as per the below staining panel in 50ul of FACS buffer for 25 min at 4C. Post staining the cells were washed twice with FACS buffer at 500g for 5min at 4C. The final pellet was resuspended in 300ul of FACS buffer with 1:1000 of 7AAD live dead staining. The cells were then taken for flow cytometric analysis.

Table 4.1. Staining marker panel for flow cytometry

Staining Panel	Cytometer Channel and Ab's					
	FITC	**PE**	**APC**	**APC-CY7**	**PE-CY7**	**PerCp/5.5**
1.	Sca1	CD45	CD95	CD90.2	CD105	7AAD
2.	MHC1	CD44	Gal9	CD45	CD24	7AAD

Tumor Cell Line Sphere Assay

Upon harvesting the tumor cells, they were immediately prepared for the sphere assay. The cells were first washed in CR-10 media to remove any residual debris or media from the harvesting process. Subsequently, the cells underwent red blood cell lysis by incubating with 500 µl of ammonium chloride potassium buffer for 5 minutes at room temperature. After lysis, the cells were washed twice with 1 ml of ice-cold PBS at 100g for 10 minutes each wash.

Following the washing steps, the cells were counted and resuspended at a concentration of 1 million cells/ml in a sphere assay medium. To initiate the sphere formation assay, 100,000 cells were seeded per well in untreated 24-well plates, with each well containing 1 ml of sphere assay medium.

Throughout the 14-day assay period, every alternate day each well received 10 µl of bFGF and EGF to support sphere growth and maintenance. On day 14, the spheres were counted under a microscope at five different high-power fields (at 12 o'clock, 3 o'clock, 6 o'clock, 9 o'clock, and the center of the well).

This entire process was repeated with tumor cells that had been cultured for 14 days prior to initiating the sphere assay. On the 14th day of culture, these cells were harvested and prepared in the same manner as described above for the freshly harvested tumor cells. The subsequent

sphere formation assay was then conducted following the same protocol.

Fludarabine/IFNγ Assay

4T1 and Py230 cells were initially seeded at a density of 100,000 cells per well in a 24-well plate. Upon reaching approximately 60% confluence, the cells were subjected to various concentrations of fludarabine: 0 µM (control), 25 µM, 50 µM, 75 µM, and 100 µM. The duration of fludarabine treatment ranged from 24 to 36 hours; prolonged exposure beyond this period resulted in observable cell death.

Following the treatment period, the cell culture media was replaced, and the cells were washed with 1x PBS to remove residual fludarabine. Fresh media was then added to allow for a recovery period of 2-3 hours. Subsequently, the cells were treated with IFNγ for 24 hours. After the IFNγ treatment, the cells were washed to remove the cytokine, followed by harvesting through trypsinization.

Post-harvesting, the cells were stained as per the previously described protocols and prepared for flow cytometric analysis.

Table 4.2. Staining marker panel for flow cytometry analysis of fludarabine assay

Staining Panel	**Cytometer Channel and Ab's**					
	FITC	**PE**	**APC**	**APC-CY7**	**PE-CY7**	**PerCp/5.5**
1.	Sca1	CD45	CD95	CD90.2	CD105	7AAD
2.	MHC1	CD44	Gal9	CD45	CD24	7AAD

Treatment with IFNg

4T1 and Py230 cells were seeded at 100,000 cells per well in a 12 well plate. Once 70% confluent, they were treated with varying concentrations of IFNg: 0U/mL, 20U/mL and

1000U/mL for 24 hours. The cells were then trypsinized and prepared for flow cytometry as described previously.

Cell counting for studying cell kinetics

Cell counting was conducted using a hemocytometer according to standard protocols. Cells were harvested and subsequently centrifuged at 500g for 5 minutes at room temperature. The resulting cell pellet was then resuspended in an appropriate volume of culture medium or buffer, ensuring thorough mixing for uniform distribution. If necessary, the cell suspension was further diluted to achieve a suitable density for counting.

To determine cell viability, 10 µL of the cell suspension was mixed with an equal volume of 0.4% trypan blue dye and loaded into the hemocytometer chamber. Cells were counted in the four large squares of the hemocytometer. The cell concentration per mL was calculated using the formula:

cell concentration per ml= (Average number of cells per large square) x (1/2) x (104).

The total cell count was then determined by multiplying the calculated cell concentration by the volume of the original cell suspension.

Bibliography

[1] Ebben, J. D., Treisman, D. M., Zorniak, M., Kutty, R. G., Clark, P. A., & Kuo, J. S. (2010). The cancer stem cell paradigm: a new understanding of tumor development and treatment. Expert Opinion on Therapeutic Targets, 14(6), 621–632. https://doi.org/10.1517/14712598.2010.485186

[2] Bracarda, S., Eggermont, A. M., & Samuelsson, J. (2010). Redefining the role of interferon in the treatment of malignant diseases. European journal of cancer (Oxford, England : 1990), 46(2), 284–297. https://doi.org/10.1016/j.ejca.2009.10.013

[3] L. Walcher, A.-K. Kistenmacher, H. Suo, R. Kitte, S. Dluczek, A. Strauß, A.-R. Blaudszun, T. Yevsa, S. Fricke, and U. Kossatz-Boehlert, "Cancer Stem Cells—Origins and Biomarkers: Perspectives for Targeted Personalized Therapies," *Frontiers in Immunology*, vol. 11, 2020, ISSN: 1664-3224. [Online].

[4] Singh, A. K., Arya, R. K., Maheshwari, S., Singh, A., Meena, S., Pandey, P., Dormond, O., & Datta, D. (2015). Tumor heterogeneity and cancer stem cell paradigm: updates in concept, controversies and clinical relevance. International journal of cancer, 136(9), 1991–2000.https://doi.org/10.1002/ijc.28804

[5] Walcher, L., Kistenmacher, A. K., Suo, H., Kitte, R., Dluczek, S., Strauß, A., Blaudszun, A. R., Yevsa, T., Fricke, S., & Kossatz-Boehlert, U. (2020). Cancer Stem Cells-Origins and Biomarkers: Perspectives for Targeted Personalized Therapies. Frontiers in immunology, 11, 1280. https://doi.org/10.3389/fimmu.2020.01280

[6] Yang, L., Shi, P., Zhao, G., Xu, J., Peng, W., Zhang, J., Zhang, G., Wang, X., Dong, Z., Chen, F., & Cui, H. (2020). Targeting cancer stem cell pathways for cancer therapy. Signal transduction and targeted therapy, 5(1), 8. https://doi.org/10.1038/s41392-020-0110-5

[7] Upadhyay G. (2019). Emerging Role of Lymphocyte Antigen-6 Family of Genes in Cancer and Immune Cells. Frontiers in immunology, 10, 819. https://doi.org/10.3389/fimmu.2019.00819

[8] He, J., Liu, Y., Zhu, T., Zhu, J., Dimeco, F., Vescovi, A. L., Heth, J. A., Muraszko, K. M., Fan, X., & Lubman, D. M. (2012). CD90 is identified as a candidate marker for cancer stem cells in primary high-grade gliomas using tissue microarrays. Molecular & cellular proteomics: MCP, 11(6), M111.010744. https://doi.org/10.1074/mcp.M111.010744

[9] Oladejo, M., Nguyen, H. M., Seah, H., Datta, A., & Wood, L. M. (2023). Tumoral CD105 promotes immunosuppression, metastasis, and angiogenesis in renal cell carcinoma. Cancer immunology, immunotherapy : CII, 72(6), 1633–1646. https://doi.org/10.1007/s00262-022-03356-5

[10] Peter, M. E., Hadji, A., Murmann, A. E., Brockway, S., Putzbach, W., Pattanayak, A., & Ceppi, P. (2015). The role of CD95 and CD95 ligand in cancer. Cell death and differentiation, 22(4), 549–559. https://doi.org/10.1038/cdd.2015.3

[11] Zhang, M., Liu, C., Li, Y., Li, H., Zhang, W., Liu, J., Wang, L., & Sun, C. (2024). Galectin-9 in cancer therapy: from immune checkpoint ligand to promising therapeutic target. Frontiers in cell and developmental biology, 11, 1332205. https://doi.org/10.3389/fcell.2023.1332205

[12] Mertowska, P., Smolak, K., Mertowski, S., & Grywalska, E. (2023). Immunomodulatory Role of Interferons in Viral and Bacterial Infections. International journal of molecular sciences, 24(12), 10115. https://doi.org/10.3390/ijms241210115

[13] Khanna NR, Gerriets V. Interferon. [Updated 2023 Jul 10]. In: StatPearls [Internet]. Treasure Island (FL): StatPearls Publishing; 2024 Jan-. Available from: https://www.ncbi.nlm.nih.gov/books/NBK555932/

[14] Platanias L. C. (2005). Mechanisms of type-I- and type-II-interferon-mediated signalling. Nature reviews. Immunology, 5(5), 375–386. https://doi.org/10.1038/nri1604

[15] Lau, J. F., & Horvath, C. M. (2002). Mechanisms of Type I interferon cell signaling and STAT-mediated transcriptional responses. The Mount Sinai journal of medicine, New York, 69(3), 156–168.

[16] Billiau, A., Heremans, H., Vermeire, K., & Matthys, P. (1998). Immunomodulatory properties of interferon-gamma. An update. Annals of the New York Academy of Sciences, 856, 22–32. https://doi.org/10.1111/j.1749-6632.1998.tb08309.x

[17] Zaidi, M. R., & Merlino, G. (2011). The two faces of interferon-γ in cancer. Clinical cancer research : an official journal of the American Association for Cancer Research, 17(19), 6118–6124. https://doi.org/10.1158/1078-0432.CCR-11-0482

[18] Schroder, K., Hertzog, P. J., Ravasi, T., & Hume, D. A. (2004). Interferon-gamma: an overview of signals, mechanisms and functions. Journal of leukocyte biology, 75(2), 163–189. https://doi.org/10.1189/jlb.0603252

[19] Alspach, E., Lussier, D. M., & Schreiber, R. D. (2019). Interferon γ and Its Important Roles in Promoting and Inhibiting Spontaneous and Therapeutic Cancer Immunity. Cold Spring Harbor perspectives in biology, 11(3), a028480. https://doi.org/10.1101/cshperspect.a028480

[20] Windbichler, G. H., Hausmaninger, H., Stummvoll, W., Graf, A. H., Kainz, C., Lahodny,

J., Denison, U., Müller-Holzner, E., & Marth, C. (2000). Interferon-gamma in the first-line therapy of ovarian cancer: a randomized phase III trial. British journal of cancer, 82(6), 1138–1144. https://doi.org/10.1054/bjoc.1999.1053

[21] Muir, A. J., Sylvestre, P. B., & Rockey, D. C. (2006). Interferon gamma-1b for the treatment of fibrosis in chronic hepatitis C infection. Journal of viral hepatitis, 13(5), 322–328. https://doi.org/10.1111/j.1365-2893.2005.00689.x

[22] Mitani, Y., Takaoka, A., Kim, S. H., Kato, Y., Yokochi, T., Tanaka, N., & Taniguchi, T. (2001). Cross talk of the interferon-alpha/beta signalling complex with gp130 for effective interleukin-6 signalling. Genes to cells : devoted to molecular & cellular mechanisms, 6(7), 631–640. https://doi.org/10.1046/j.1365-2443.2001.00448.x

[23] Kasahara, T., Hooks, J. J., Dougherty, S. F., & Oppenheim, J. J. (1983). Interleukin 2-mediated immune interferon (IFN-gamma) production by human T cells and T cell subsets. Journal of immunology (Baltimore, Md. : 1950), 130(4), 1784–1789.

[24] Jorgovanovic, D., Song, M., Wang, L., & Zhang, Y. (2020). Roles of IFN-γ in tumor progression and regression: a review. Biomarker research, 8, 49. https://doi.org/10.1186/s40364-020-00228-x

[25] Czarniecki, C. W., & Sonnenfeld, G. (2006). Clinical Applications of Interferon-γ. The Interferons: Characterization and Application, 309-336.

[26] Zhang, L., Wu, H., Lu, D., Li, G., Sun, C., Song, H., Li, J., Zhai, T., Huang, L., Hou, C., Wang, W., Zhou, B., Chen, S., Lu, B., & Zhang, X. (2013). The costimulatory molecule B7-H4 promote tumor progression and cell proliferation through translocating into nucleus. Oncogene, 32(46), 5347–5358. https://doi.org/10.1038/onc.2012.600

[27] Jing, Z. L., Liu, G. L., Zhou, N., Xu, D. Y., Feng, N., Lei, Y., Ma, L. L., Tang, M. S., Tong, G. H., Tang, N., & Deng, Y. J. (2024). Interferon-γ in the tumor microenvironment promotes the expression of B7H4 in colorectal cancer cells, thereby inhibiting cytotoxic T cells. Scientific reports, 14(1), 6053. https://doi.org/10.1038/s41598-024-56681-3

[28] Ricci, F., Tedeschi, A., Morra, E., & Montillo, M. (2009). Fludarabine in the treatment of chronic lymphocytic leukemia: a review. Therapeutics and clinical risk management, 5(1), 187–207. https://doi.org/10.2147/tcrm.s3688

[29] Baran-Marszak, F., Feuillard, J., Najjar, I., Le Clorennec, C., Béchet, J. M., Dusanter-Fourt, I., Bornkamm, G. W., Raphaël, M., & Fagard, R. (2004). Differential roles of STAT1alpha and STAT1beta in fludarabine-induced cell cycle arrest and apoptosis in human B cells. Blood, 104(8), 2475–2483. https://doi.org/10.1182/blood-2003-10-3508

[30] Frank, D. A., Mahajan, S., & Ritz, J. (1999). Fludarabine-induced immunosuppression is associated with inhibition of STAT1 signaling. Nature medicine, 5(4), 444–447. https://doi.org/10.1038/7445

[31] Xiu, H., Gong, J., Huang, T., Peng, Y., Bai, S., Xiong, G., Zhang, S., Huang, H., Cai, Z., & Zhang, G. (2021). Fludarabine inhibits type I interferon-induced expression of the SARS-CoV-2 receptor angiotensin-converting enzyme 2. Cellular & molecular immunology, 18(7), 1829–1831. https://doi.org/10.1038/s41423-021-0